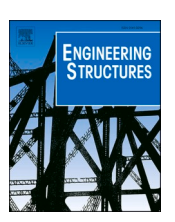
ELSEVIER

Contents lists available at ScienceDirect

Engineering Structures

journal homepage: www.elsevier.com/locate/engstruct





Cyclic experiments on isolated steel sheet connections for CFS framed steel sheet sheathed shear walls with new configurations

Zhidong Zhang ^{a,*}, Amanpreet Singh ^b, Fani Derveni ^c, Shahabeddin Torabian ^a, Kara D. Peterman ^c, Tara C. Hutchinson ^b, Benjamin W. Schafer ^a

- a Department of Civil and Systems Engineering, Johns Hopkins University, 3400 North Charles Street, Baltimore, MD 21218, United States
- ^b Department of Structural Engineering, University of California, San Diego, La Jolla, CA 92093, United States
- c Department of Civil and Environmental Engineering, University of Massachusetts, Amherst, 130 Natural Resources Road, Amherst, MA 01003, United States

ARTICLE INFO

Keywords: Earthquake engineering Cold-formed steel Steel sheet sheathed shear walls Fastener shear connections Cyclic testing

ABSTRACT

The main objective of this research is to experimentally characterize the performance of isolated single sheathing-to-framing fastener connections under cyclic load as utilized in emerging classes of cold-formed steel (CFS) framed steel sheet sheathed shear walls used for seismic lateral resistance. New shear wall variations include the use of steel sheet sheathing sandwiched between framing members (i.e., mid-ply) and the use of heavy hollow structural sections (HSS) chord members with the thin steel sheet sheathing attached by power actuated fasteners (PAF) to the HSS. The cyclic nonlinear response of the framing to steel sheet fastener connection is fundamental for simulating the seismic performance of steel sheet sheathed shear walls. Minimal cyclic fastener-level test data under shear exists for these new configurations. A unique lap shear test following AISI S905 was designed to study and characterize the cyclic fastener connection behavior. The specimens were loaded with an asymmetric cyclic loading protocol which intentionally buckles the thin sheet in the compression direction, and progressively increases in the tension direction. Sixty-three tests covering a wide range of framing thickness, sheet thickness, fastener type and size were completed. Each connection configuration is characterized with a multi-linear backbone curve ready for use in numerical shear wall models. The tested fastener configurations exhibit excellent performance as fastener tilting is largely or completely eliminated in these configurations, and connection degradation from buckling of the steel sheet is minimized. It is also shown that AISI S100 connection strength provisions are applicable to the tested connections.

1. Introduction

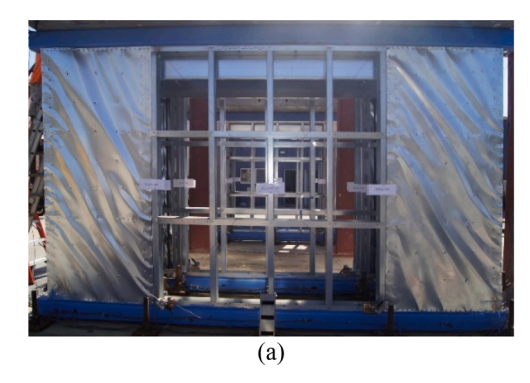
The need for low cost, multi-hazard resilient, sustainable, light-weight building structures can be potentially fulfilled by cold-formed steel (CFS) framed structures. One of the primary structural components providing lateral resistance in CFS-framed structures is the CFS-framed steel sheet sheathed shear wall [1]. A CFS framed steel sheet sheathed shear wall consists of steel sheet sheathing, CFS studs, CFS tracks, blocking members, hold-downs or tie rods, and fasteners connecting the framing and steel sheet sheathing. Post testing photographs of a wall line consisting of two standard configuration steel sheet sheathed shear walls and an interior gravity wall tested on a shake table in another related study by the authors [2] are shown in Fig. 1. Shear buckling waves in the steel sheet sheathing as shown in Fig. 1(a) were

easily observed as the dominant feature. But, peak strength and postpeak behavior are controlled largely by fastener connection failure as shown in Fig. 1(b). The cyclic nonlinear response of the fastener connection is particularly significant for the overall shear wall response, and the impact of the steel sheet shear buckling on the connection behavior needs to be considered.

Recent CFS framed steel sheet sheathed shear wall tests at McGill University have examined the impact of new shear wall configuration sandwiching the thin steel sheet between thick boundary members (i.e., mid-ply) [3–6]. This new configuration demonstrates the potential of higher shear capacity and ductility necessary in mid-rise CFS construction. Post testing photographs of a representative mid-ply steel sheet sheathing shear wall test [3] are presented in Fig. 2. Shear rupture failure is accompanied by the steel sheet sheathing shear buckling in this

E-mail addresses: zhidongzhang@jhu.edu (Z. Zhang), ams082@eng.ucsd.edu (A. Singh), fderveni@umass.edu (F. Derveni), torabian@jhu.edu (S. Torabian), kdpeterman@umass.edu (K.D. Peterman), tara@ucsd.edu (T.C. Hutchinson), schafer@jhu.edu (B.W. Schafer).

^{*} Corresponding author.



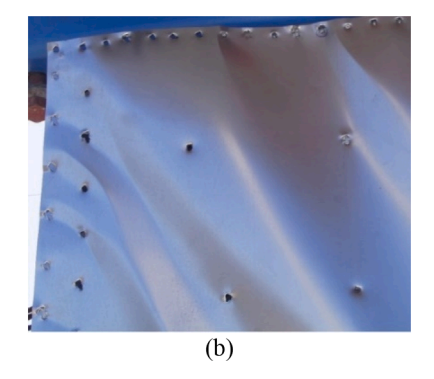


Fig. 1. Post-test photographs of a previously tested CFS framed steel sheet sheathed shear wall line shake table test from [2]. (a) Shear buckling waves in the steel sheet sheathing, (b) Fastener connection failure.





Fig. 2. Post testing photographs of a mid-ply steel sheet sheathed shear wall test and steel sheet sheathing failure [3]. (a) Shear wall test, (b) Shear rupture incorporating steel sheet shear buckling.

test, as presented in Fig. 2(b). Adopting hollow structural sections (HSS) steel components as the load bearing studs is a reasonable solution to fulfill the demands on the shear walls in multi-story buildings both in terms of gravity load as well as overturning and overstrength requirements. It is necessary and of great interest to study the cyclic connection behavior incorporating steel sheet sheathing buckling of CFS framed steel sheet shear walls with new configurations including midply sheathing and HSS chord stud configurations.

The limited existing test data on the connections of CFS framed steel sheet sheathed shear walls with new configuration [6-11] is shown in Table 1. These tests include cyclic and monotonic performance of

connection configurations subject to single shear (denoted as "SS") with #12 self-drilling screw, Power Actuated Fastener (PAF), thin steel sheet, and thick steel plate the same thickness as a common HSS section. Additionally, a series of monotonic tests on connection configurations subject to double shear (denoted as "DS") with #8, #10, #12 screw, steel sheet and framing steel with various thickness are also summarized in Table 1. No cyclic connection tests with two framing plies sandwiching the thin steel sheet appropriate for mid-ply steel sheet sheathing shear walls and limited single shear cyclic connection tests with framing steel plate ply the same thickness as HSS exist.

The strength of CFS framed steel sheet sheathed shear walls is established in AISI S400-15 [12] in North America, which provides three methods: (i) experimentally tabulated values, (ii) an "effective strip method" [13] empirically considering tension field action and connection strength limit, and (iii) application of the principles of mechanics and supplemental data. The strength of a limited number of CFS-framed steel sheet sheathed shear walls with standard configurations can be established with method (i). The connection strength, typically necessary for methods (ii) and (iii) is provided in AISI S100-16 [14]. Accurate knowledge of the connection level behavior provided in AISI S100-16 is necessary for determining the shear wall strength of cases with new configurations using the "effective strip method" or the principles of mechanics and supplemental data.

The objectives of the testing program on steel-to-steel connections in shear is to (i) provide results appropriate for CFS framed steel sheet sheathed shear walls with new configurations incorporating the impact of steel sheet shear buckling on the connection, (ii) characterize the connection performance and establish baseline behavior, and (iii) evaluate the current code provisions' applicability for these connection configurations. A unique cyclic lap shear testing configuration, following AISI S905-13 [15], demonstrating either one thin steel sheet ply and two thick framing plies or one thin steel sheet ply and one thick framing ply connected by one single fastener was designed and built.

 Table 1

 Summary of relevant available fastener connection tests.

Source	Shear	Load Type	Fastener	Ply 1* (mm)	Ply 2** (mm)
Shi et al. [7]	SS	Cyclic & Monotonic	PAF	0.69, 1.09	4.78
			#12	0.69, 1.09	4.78
Torabian et al. [8,9]	SS	Cyclic & Monotonic	PAF	0.69, 0.84, 1.09	4.78
Daudet et al. [10]	DS	Monotonic	#12	0.84	0.84
				1.09	1.09
				1.37	1.37
Koka et al. [11]	DS	Monotonic	#10	0.43	0.43
				0.74	0.74
Wu [6]	DS	Monotonic	#8	0.36, 0.47	2.46
			#10	0.36, 0.47, 0.84, 1.09	2.46
			#12	0.84, 1.09	2.46

^{*} Ply 1 is the steel sheet ply in contact with fastener head in the single shear configuration while it is the mid-ply in the double shear configuration.

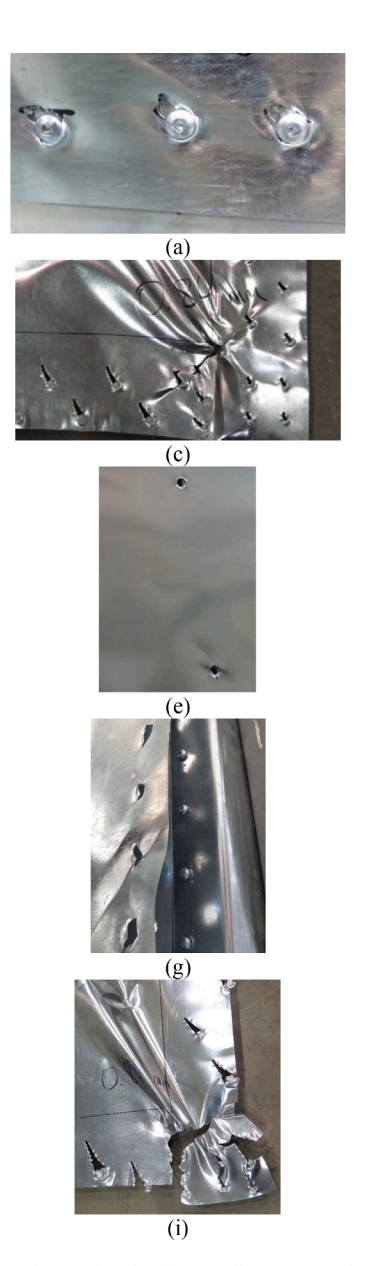
^{**} Ply 2 refers the steel sheet plies other than Ply 1 within the fastener connections.

Since a small magnitude of compressive displacement will trigger the steel sheet ply to buckle and the maximum compression strength is reached, a small compressive displacement is adequate to study the steel sheet buckling effects on the fastener connection's behavior and capture the connection strength under compression. The cyclic loading protocol adopted herein is asymmetric with a small displacement applied in the compressive direction which buckles the thin steel sheet followed by progressively larger displacements in the tensile direction. The test data are characterized with a multi-segment linear backbone phenomenological model to support the design and simulation for CFS-framed steel sheet sheathed shear walls with new configurations. The experimental details and processing of sixty-three tests on steel sheet connections for CFS framed steel sheet sheathed shear walls with new configurations are provided in this paper.

2. Fastener connection failure modes

Fastener connection failure mode is as important as connection strength in design. The fastener failures observed in the shear wall tests

[3–6] and idealized failure mechanisms are summarized in Fig. 3. The primary mode of behavior observed in this testing program is bearing without tilting since the dominant demand on the connection is either double sided shear or single sided shear with thick framing steel ply configuration, as shown in Fig. 3(a), 3(b), 3(c), 3(d). However, disengagement of the framing and steel sheet is the ultimate failure mode and pull-through, pull-through with bearing, and shear rupture failure modes are also commonly observed in the shear wall tests with new configurations. Pull-through and pull-through with bearing are primarily associated with tensile demand on the single sided shear connections while shear rupture (or edge tear out) is associated with shear demand on both single and double sided shear connections. Pullthrough, as shown in Fig. 3(e) and Fig. 3(f), is not specifically defined in AISI S100-16 [14], but is close in behavior to pull-over. Pull-through develops when the stud or track flange deforms and pulls the fastener with it resulting in the fastener head tearing through the sheet. If obvious twisting is involved in the stud or track deformation then the failure mode is pull-through with bearing when the connection is loaded under single sided shear with thick framing steel ply configuration, as



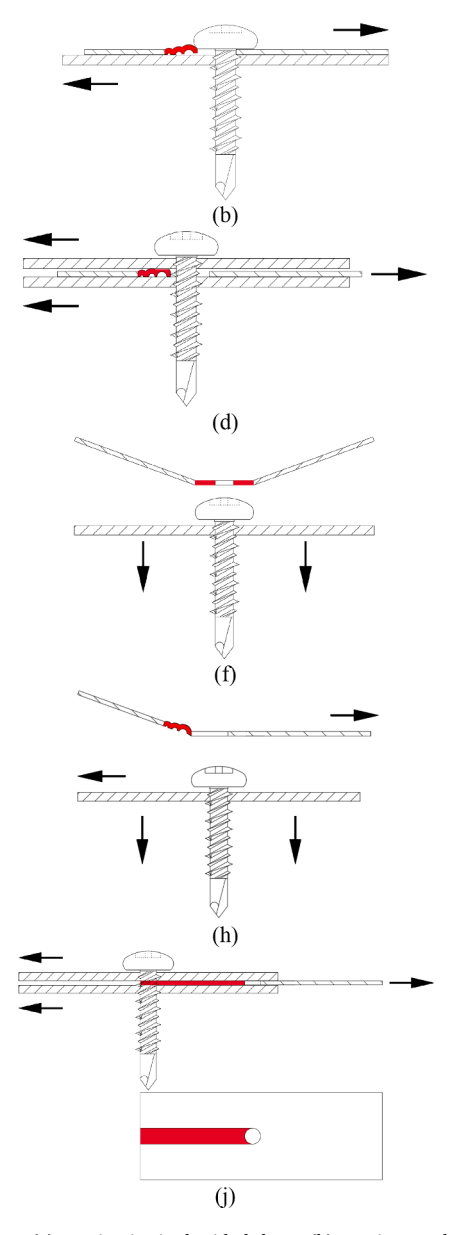


Fig. 3. Fastener failures observed in the shear wall tests [3] and idealized failure mechanism. (a) Bearing in single sided shear, (b) Bearing mechanism in single sided shear, (c) Bearing in double sided shear, (d) Bearing mechanism in double sided shear, (e) Pull-through, (f) Pull-through mechanism, (g) Pull-through with bearing, (h) Pull-through with bearing mechanism, (i) Shear rupture in double sided shear, (j) Shear rupture mechanism in double sided shear.

shown in Fig. 3(g) and Fig. 3(h). Shear rupture failures develop because of minimal edge distance limiting the bearing capacity, shear rupture happening in a double sided shear connection is presented in Fig. 3(i) and Fig. 3(j).

3. Experimental program

3.1. Test matrix

The selected fastener type and size, sheet ply thicknesses in this connection testing program are provided in Table 2. Taking both the existing fastener connection test data in Table 1 and shear wall test data with new configuration [3–6] into account and covering a wide range of steel sheet thickness, fastener type and size, and various loading types, the test matrix is designed. Double sided shear configuration specimens (DS) demonstrating one thin steel sheet sandwiched by two CFS framing steel plies (in contact with the fastener head) represent steel sheet sheathed shear walls with boundary members sandwiching the steel sheet sheathing (i.e., mid-ply). Single sided shear configuration connections (SS) with steel plates as thick as common HSS sections and self-drilling screws or PAFs are aimed at investigating the behavior of fasteners in CFS framed steel sheet sheathed shear walls with stiffer framing configuration.

Seven tests including a monotonic test, three asymmetric cyclic tests with thin sheet buckling away from the fastener head, and three asymmetric cyclic tests with thin sheet buckling towards the fastener head are carried out for each connection configuration, as presented in Table 2. The necessity to investigate the thin sheet buckling directions lies in that obvious strength difference was found in some standard single shear connection configuration tests when sheet thickness and framing thickness are close in the complete test report [16]. Each test series is assigned a unique name according to an established nomenclature: e.g., the "97-12-30-97" series, stands for two 2.46 mm (97 mil) thick framing steel plies sandwiching a 0.76 mm (30 mil) thin steel sheet ply connected by a single #12 self-drilling pan head screw. Single sided shear configuration test series, for example, "188-24-30" implies a 0.76 mm (30 mil) thin steel sheet ply and a 4.78 mm (188 mil) framing steel ply are fastened by a single Hilti Power-Actuated Fastening X-HSN-24 fastener (X-ENP-19 represented with "19" is adopted in other single sided shear test series). Each test conducted is given a unique test number "test IDtest series name-load type" where load type "M", "A", and "T" represents monotonic tests, asymmetric cyclic tests with thin steel sheet buckling away from and towards the fastener head respectively. All individual test results are provided in the complete test report with consistent nomenclature in this paper [16]. Table 2 is grouped using solid horizontal lines, the test series grouped demonstrate the same sheet and framing thickness. Comparison between test series within the same group can study the effects of fastener on the connection behavior. These various groups are able to cover single or double shear configurations and different sheet and framing thickness level.

3.2. Test specimens

The steel sheet sheathing buckling behavior and resulting fastener connection failure are not currently captured by the standard lap-joint shear test specimen configuration per AISI S905-13 [15]; therefore, the test specimen must be specially designed based on the failure modes observed in shear wall tests as shown in Fig. 3 and previously detailed. The perimeter fastener connections in the shear walls not only resist shear demand but also need to resist out-of-plane forces that acts on the fastener head due to thin steel sheet sheathing extensive shear buckling. The force caused by the sheet buckling can lead to premature pull-through behavior in contrast to pure bearing in a connection even though itself is not a large demand. This "shear-tension" interaction is identical for the fastener connection behavior and the overall shear wall response under seismic events.

Dimensions and loading protocol of a standard lap shear joint test were modified in this testing program to provide these additional conditions. A single sided shear configuration specimen is shown in Fig. 4 (a), the upper and bottom shaded parts with 50.8 mm length are clamping areas for the grips, 50.8 mm x 50.8 mm spacers are put inside the grips to avoid eccentric loading. The thin steel sheet ply length is equal to the buckling half-wave length of steel sheet sheathing adjacent to the shear wall framing boundary. After reviewing some typical steel sheet shear buckling half-waves at the perimeter in the shear wall tests which are marked with parallel red lines in Fig. 5, a simple estimate for the shear buckling half-wave length at the perimeter is 101.6 mm. This distance then corresponds to the length between the top grip and fastener head of the specimen. The thin steel sheet ply edge distance is chosen to be 19.1 mm which fulfills the requirement that edge distance should be not less than one and a half nominal fastener diameter per J4.2 in AISI S100-16 [14] for all tests. The edge distance of the thick framing ply is set equal to 20.6 mm which corresponds to half of the flange width of a typical chord stud section (362S162-97). The length between the bottom grip and fastener is 25.4 mm minimizing tilting of the steel ply in a standard lap-joint shear test based on AISI S905-13 [15]. The double sided shear configuration specimen, as presented in Fig. 4(b), demonstrates the same geometric size as the single sided shear configuration specimen. There are two thick framing plies and one spacer put between them. The specimens were assembled in the Thin-walled Structures Laboratory at Johns Hopkins University. A pilot hole was adopted for all the specimens with self-drilling screws and a HILTI ST 1800 screw gun with a torque setting between 12 to 15N.m was utilized to assemble specimens. Appropriate caliber cartridges and automatic poweractuated tool settings per the user manual were set up to obtain the PAF manufacturers' recommended nail head standoff distances.

3.3. Test setup

The test rig is shown in Fig. 6(a). All the tests were conducted in an MTS servohydraulic test system. A position transducer (PT) and a load cell are employed to acquire deformation and force data. In addition, a

Table 2Proposed matrix for steel framing-to-steel sheet fastener test.

Test series	Shear	Fastener	d* (mm)	Sheet (mm)	Sheet f_{yn} (MPa)	Framing (mm)	Framing f_{yn} (MPa)	Mon test #	Cyclic test #
97-10-13-97	DS	#10	4.75	0.33	345	2.46	345	1	6
97-10-19-97	DS	#10	4.75	0.48	227	2.46	345	1	6
97-10-30-97 97-12-30-97 97-24-30-97	DS DS DS	#10 #12 X-HSN-24	4.75 5.38 4.04	0.76 0.76 0.76	227 227 227	2.46 2.46 2.46	345 345 345	1 1 1	6 6 6
118-24-30-118	DS	X-HSN-24	4.04	0.76	227	3.00	345	1	6
188-12-30 188-24-30	SS SS	#12 X-HSN-24	5.38 4.04	0.76 0.76	227 227	4.78 4.78	345 345	1 1	6 6
375-19-30	SS	X-ENP-19	4.45	0.76	227	9.53	345	1	6

^{*} d is the measured diameter for fasteners.

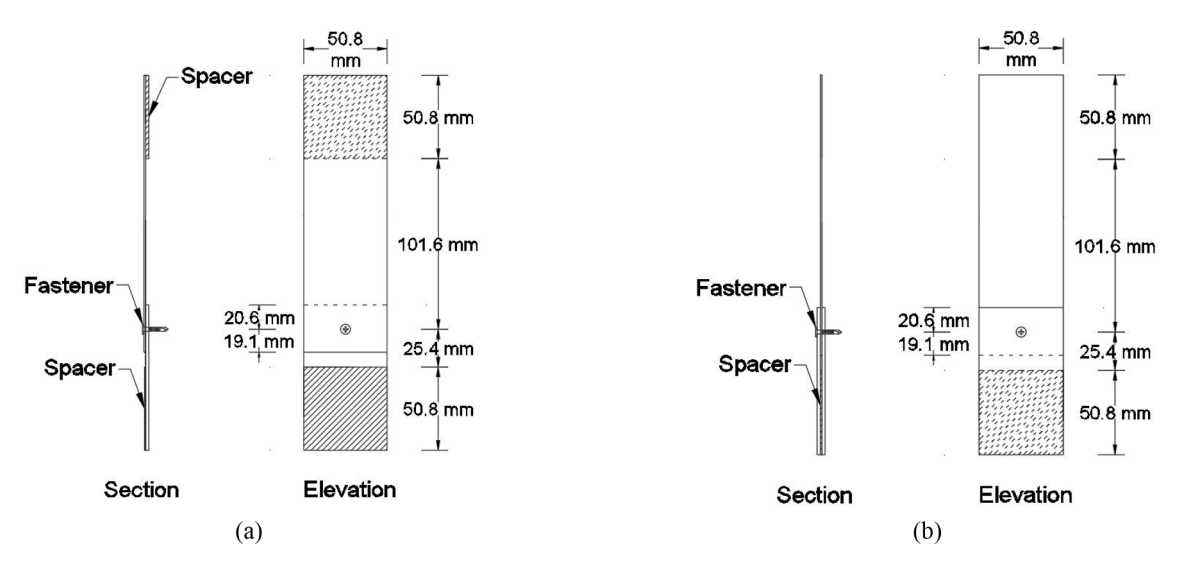


Fig. 4. Typical test specimens. (a) Single sided shear configuration specimen, (b) Double sided shear configuration specimen.

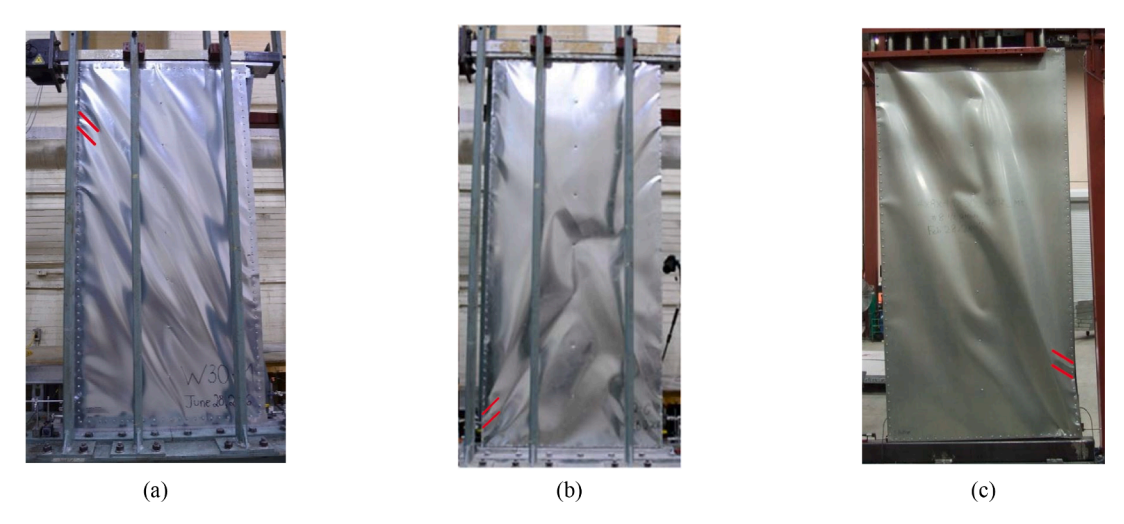


Fig. 5. Typical steel sheet shear buckling half-waves at the perimeter in the shear wall tests. (a) [4,5], (b) [17], (c) [18].

laser displacement sensor is utilized to monitor the out-of-plane thin steel sheet buckling deformation. A mechanical lateral support was installed at either left or right side to lead the thin sheet to buckle away or towards the fastener head. Fig. 6(b) and Fig. 6(c) show typical single sided shear and double sided shear configuration specimens in the test rig. Fig. 6(d) and Fig. 6(e) depict the typical specimen's response in tension and compression. The positive displacement side of the forcedisplacement curve provides the bearing stiffness and connection strength in shear for the specimen under tension while the negative displacement side of the force-displacement curve reflects the thin steel sheet buckling strength when the specimen is in compression. Since previous cyclic testing demonstrates that the response is symmetric [6-9,19], one-sided cyclic lap shear testing is able to investigate the shear behavior. The buckling of the thin steel sheet is able to create a shear-tension interaction on the fastener connection, maximizing the opportunity that the fastener tilts and slips through the thin steel sheet for the single sided shear configuration specimens.

3.4. Loading protocol

The FEMA 461 Quasi-Static loading protocol [20] was implemented by the previous CFS fastener connection cyclic shear tests [6–9,19]. This loading protocol is adopted and modified to incorporate a small magnitude of compression displacement: 2.54 mm is estimated using a

sine wave approximation for the buckling wave [16] with out-of-plane buckling deformation equal to 10.2 mm based on the shell finite element simulation of steel sheet shear walls in ABAQUS [21]. As presented in Fig. 7, the modified FEMA 461 loading protocol demonstrates two repeated symmetric cycles increasing in magnitude by a factor of 1.4 until the compression displacement exceeds 2.54 mm. The tension side of subsequent two repeated asymmetric cycles features magnitude increase by a factor of 1.4 while the compression side keeps constant maximum displacement 2.54 mm. A 0.028 mm/sec loading rate is employed in the initial six cycles while 0.084 mm/sec loading rate is adopted for the later cycles. Following AISI S905-13 [15], 0.021 mm/sec loading rate is implemented for the monotonic tests.

4. Test results

4.1. Material properties

The material testing contains three standard tensile coupons per ASTM E8/E8M-13a [22] for each thickness of sheet material. The zinc coating at the two ends of the coupon was stripped with Hydrochloride acid (HCL-1N) for the accurate measurement of base metal thickness [23]. The coupons were loaded at a rate of 0.021 mm/sec. Representative engineering stress strain curves for each thickness level are selected and plotted in Fig. 8 for direct comparison. The averaged test

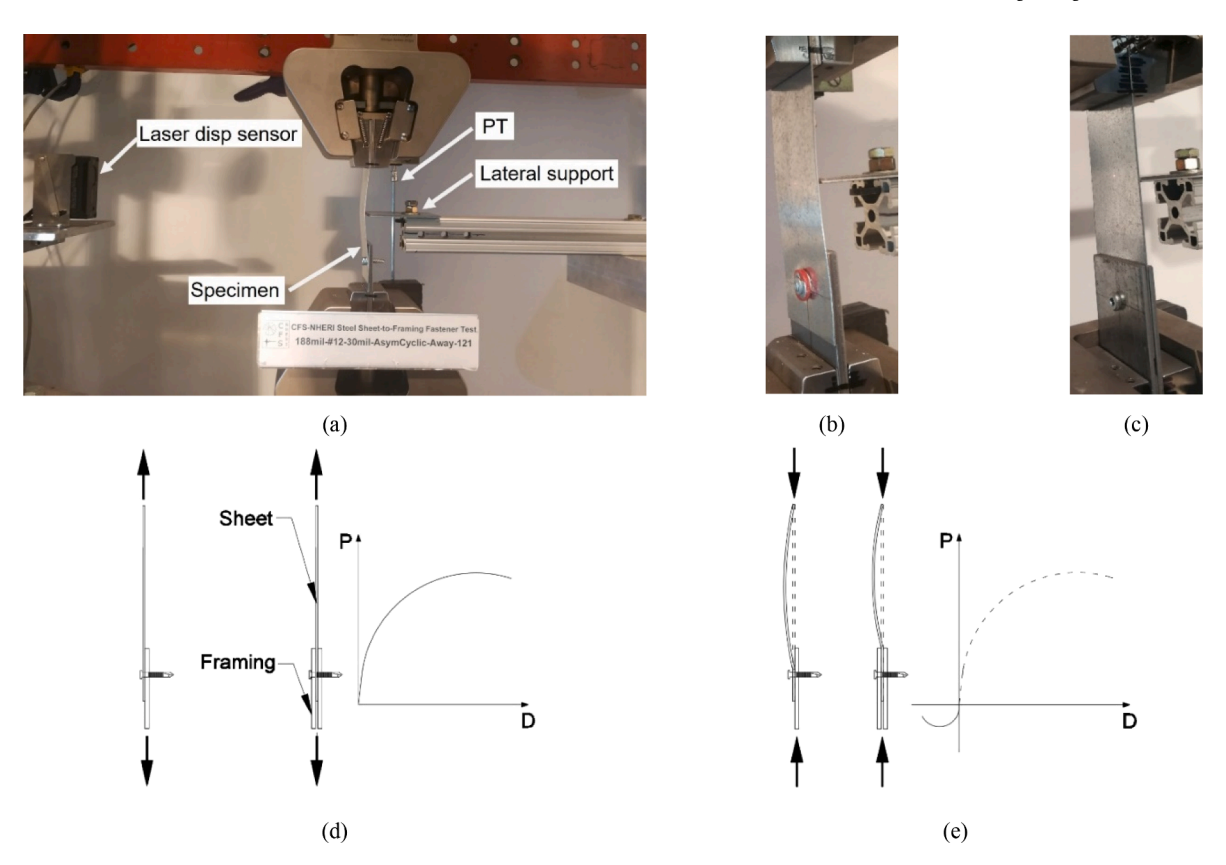


Fig. 6. Test rig and specimen. (a) Test setup, (b) Single sided shear test specimen in the test rig, (c) Double sided shear test specimen in the test rig, (d) Test specimen response in tension, (e) Test specimen response in compression.

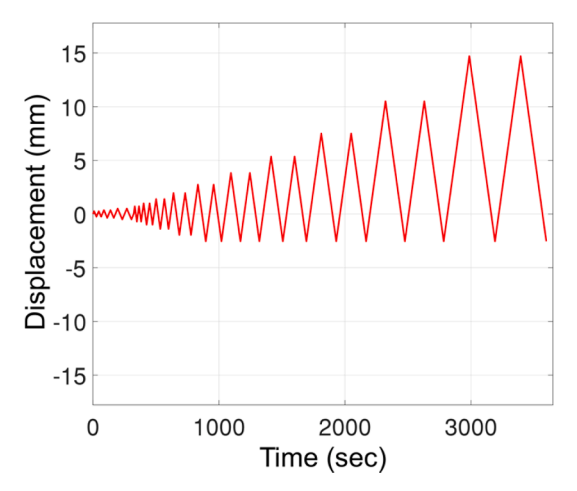


Fig. 7. Asymmetric cyclic loading protocol.

results including yielding stress $f_{0.2}$ (0.2% offset method), tensile strength $f_{\rm tb}$, strain at tensile $\varepsilon_{\rm tb}$, and the total elongation ratio $\varepsilon_{\rm r}$ are summarized in Table 3. Note that the thick steel plate material properties were not tested and nominal yielding strength 345 MPa and tensile strength 450 MPa are employed when calculating the connection shear strength per AISI S100 provisions [14] in the later code strength prediction discussion. The tested yielding stress of 0.33 mm, 0.48 mm, and 0.76 mm thin sheet material are lower than the nominal yielding stress especially the 0.76 mm thin sheet material. The tested yielding stress of 2.46 mm, 3.00 mm thin sheet material are higher than the nominal yielding stress. The 0.48mm and 0.76mm thin sheet materials tend to show low yield stress and high elongation aligning well with the CFS framed steel sheet sheathed shear wall design philosophy that the steel

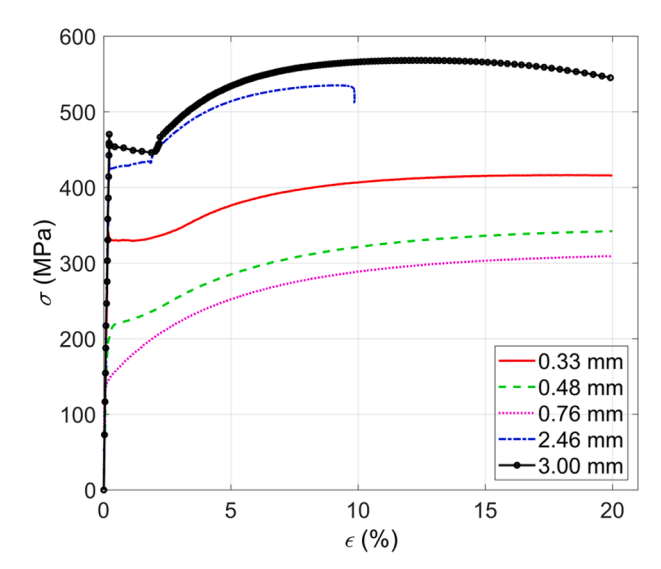


Fig. 8. Representative engineering stress strain curves from steel sheet material.

sheet sheathing works as an energy dissipating fuse with lower yield stress and higher ductility.

4.2. Result summary

Key cyclic test result statistics averaged by test series and monotonic test result for each test series, both double shear (DS) and single shear (SS) are summarized in Table 4. The initial stiffness k_0 is evaluated based on the response at 40% of the peak strength (P_{peak}) consistent with AISI

Table 3
Material test result.

Nominal Thickness (mm)	Measured Thickness (mm)	f _{yn} (MPa)	f _{0.2} (MPa)	f _u (MPa)	ε _u * (%)	ε _r ** (%)
0.33	0.31	345	332.4	415.8	17.6	26.4
0.48	0.48	227	209.0	343.7	21.8	41.0
0.76	0.78	227	150.4	312.1	22.3	46.0
2.46	2.54	345	422.4	534.2	10.8	16.2
3.00	3.11	345	449.5	564.5	12.9	21.6

 $^{^*}$ Strain at tensile ε_u , is achieved using an extensometer with 25.4 mm gauge length and 5.1 mm maximum range.

test standards (AISI S907 [24], AISI S917 [25]). Deformation at the peak strength level is denoted as $D_{\rm peak}$ while deformation at the 80% postpeak force level is expressed as $D_{80\%}$. The peak strength is significantly affected by sheet thickness and whether the connection is in single shear or double shear with fastener type and size playing secondary roles. The connection stiffness is consistently higher in those specimens with the X-HSN-24 PAF, indicating excellent initial connection in those configurations. A few monotonic test results demonstrate large difference than the corresponding averaged cyclic test result especially the initial stiffness k_0 because we only conduct one monotonic test for each test series which may cause outlier data. The coefficient of variation (CoV) is overall low except the "188-12-30" test series because tests with different thin sheet buckling directions trigger variability in failure modes and connection strength.

4.3. Typical deformation and failure modes

Predominant failure modes observed in the testing are bearing, shear rupture and pull-through with bearing. Bearing is observed previous to disengagement caused by either shear rupture or pull-through with bearing. The pull-through with bearing failure mode, as depicted in Fig. 3(h), occurs only after bearing has been initiated and is accompanied by tearing of the thin steel sheet ply area in contact with the fastener head in the single sided shear connection. There will be a plastic

hinge in the middle of the thin steel sheet after a small number of compression cycles. The deformation and failure development are carefully observed in each test. Note that the subsequent images are selected as close as possible to the exact force levels.

The "97-12-30-97" test series is selected as a representative for double sided shear connection tests. The deformation and failure development of a test in the "97-12-30-97" test series are presented in Fig. 9, demonstrating bearing and shear rupture failure which is obviously observed in the red rectangle areas in the Fig. 9(d) and 9(e). The thin steel sheet ply is constrained to buckle away from the fastener head in compression. No tilting is observed since the double sided shear connection does not generate eccentric forces and there is no obvious deformation in the two thick 2.46 mm framing steel plies. Most double sided shear connection tests exhibit similar overall deformation and failures.

The similar deformation and failure development are observed in single sided shear connections with PAF. The deformation and failure development of a test in the "188-24-30" test series are presented in Fig. 10. The thin steel sheet ply is constrained to buckle away from the fastener head in this test. Tilting is not captured since the thick steel plate is stiff and the moment-resisting arm of PAF head is larger than typical screws. Bearing failure is observed at the peak strength level which is shown in the rectangle area in the Fig. 10(b) and the bearing progresses throughout the testing. Shear rupture is obviously presented in Fig. 10(d) and 10(e). The demand on the fastener is mainly shear with minimal tension. Bending of the thin steel sheet ply is initialized by the PAF and progresses throughout the test. No deformation is observed in the 4.78 mm steel plate.

The similar behavior is captured in two tests of single sided shear connection with self-drilling screw test series "188-12-30" with higher connection strength, but most tests in this test series demonstrate pull-through with bearing failure and shear rupture failure after bearing failure initiates. A test in the "188-12-30" test series is chosen as a representative, whose deformation and failure development is shown in Fig. 11. The thin steel sheet ply is constrained to buckle away from the fastener head. No screw tilting is captured since the thick steel plate is stiff. Bearing in the thin ply is the primary failure and it can be observed at the peak force level which is indicated with a red rectangle in Fig. 11

Table 4
Monotonic test and averaged cyclic test results.

Test series	S^1	Sheet (mm)	F^2	Framing (mm)	L^3	k_0 (kN/m	ım)	D _{peak} (m	n)	P_{peak} (k	N)	$D_{80\%}$ (m)	m)
						Avg ⁴	CoV	Avg	CoV	Avg	CoV	Avg	CoV
97-10-13-97	DS	0.33	#10	2.46	M	43.78	_	3.40	_	2.78	-	6.30	_
					C	8.66	0.59	3.80	0.13	2.58	0.03	6.89	0.06
97-10-19-97	DS	0.48	#10	2.46	M	3.73	-	7.37	-	3.31	-	9.25	_
					C	4.59	0.51	8.53	0.08	3.46	0.01	10.87	0.04
97-10-30-97	DS	0.76	#10	2.46	M	3.77	_	9.68	_	4.79	-	11.99	-
					C	5.89	0.25	9.38	0.05	5.02	0.03	12.45	0.05
97-12-30-97	DS	0.76	#12	2.46	M	5.83	-	9.60	-	5.19	-	12.55	-
					C	6.12	0.29	10.01	0.05	5.33	0.03	13.58	0.03
97-24-30-97	DS	0.76	P2	2.46	M	41.07	-	9.93	-	5.22	-	13.36	-
					C	34.21	0.09	9.56	0.06	4.85	0.06	13.50	0.03
118-24-30-118	DS	0.76	P2	3.00	M	25.57	-	10.29	_	4.87	-	14.27	_
					C	31.51	0.21	9.89	0.05	5.07	0.08	13.78	0.04
188-12-30	SS	0.76	#12	4.78	M	57.44	_	1.45	_	3.65	-	5.13	-
					C	13.91	0.25	4.19	0.53	3.41	0.23	6.62	0.23
188-24-30	SS	0.76	P2	4.78	M	36.86	_	3.91	-	4.68	_	6.99	_
					C	40.53	0.17	5.77	0.29	4.89	0.04	8.95	0.16
375-19-30	SS	0.76	P1	9.53	M	20.01	_	4.17	_	5.08	_	6.91	_
					C	12.11	0.22	5.29	0.13	4.67	0.05	7.77	0.13

¹ SS is single shear connection configuration while DS is double shear connection configuration.

 $^{^{**}}$ Total elongation ratio $\varepsilon_{\rm r}$ is based on the measured distance between two manually drawn lines before testing with 5.1 mm gauge length.

² P1 implies X-ENP-19 PAF while P2 means X-HSN-24 PAF.

³ M is monotonic and C is cyclic.

⁴ Avg implies the averaged value for all the cyclic tests in each test series or single one monotonic test value.

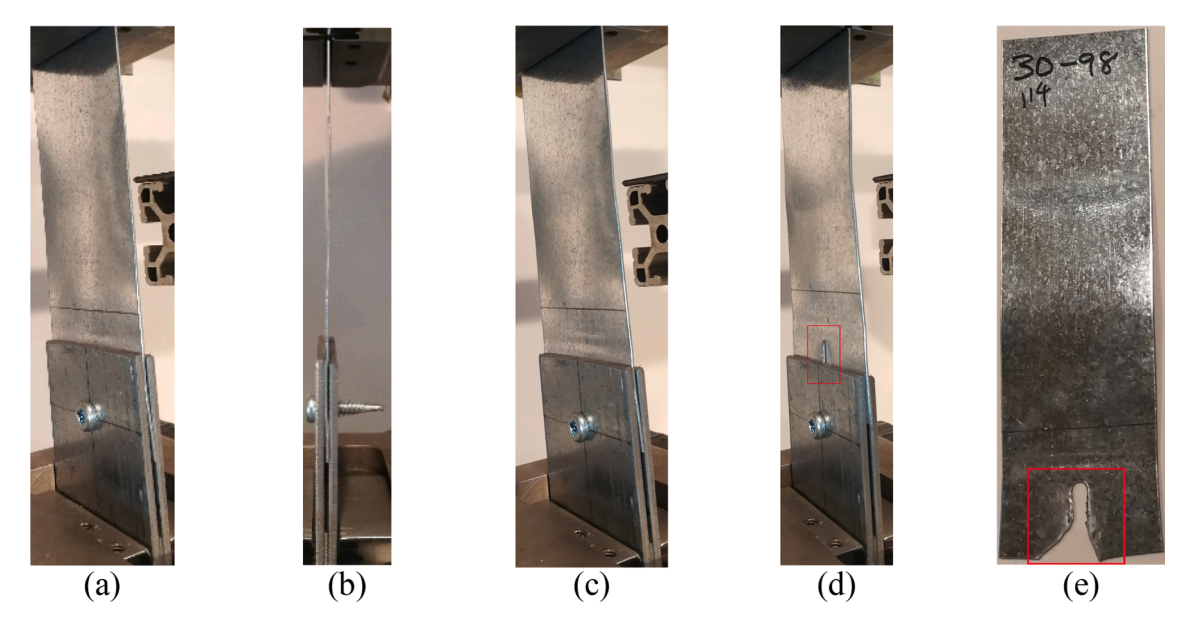


Fig. 9. Deformation and failure of a test in the "97-12-30-97" test series. (a) Peak strength level front view, (b) Peak strength level side view, (c) 80% post-peak strength level, (d) Post-test front view, (e) Post-test mid-ply face-on view.

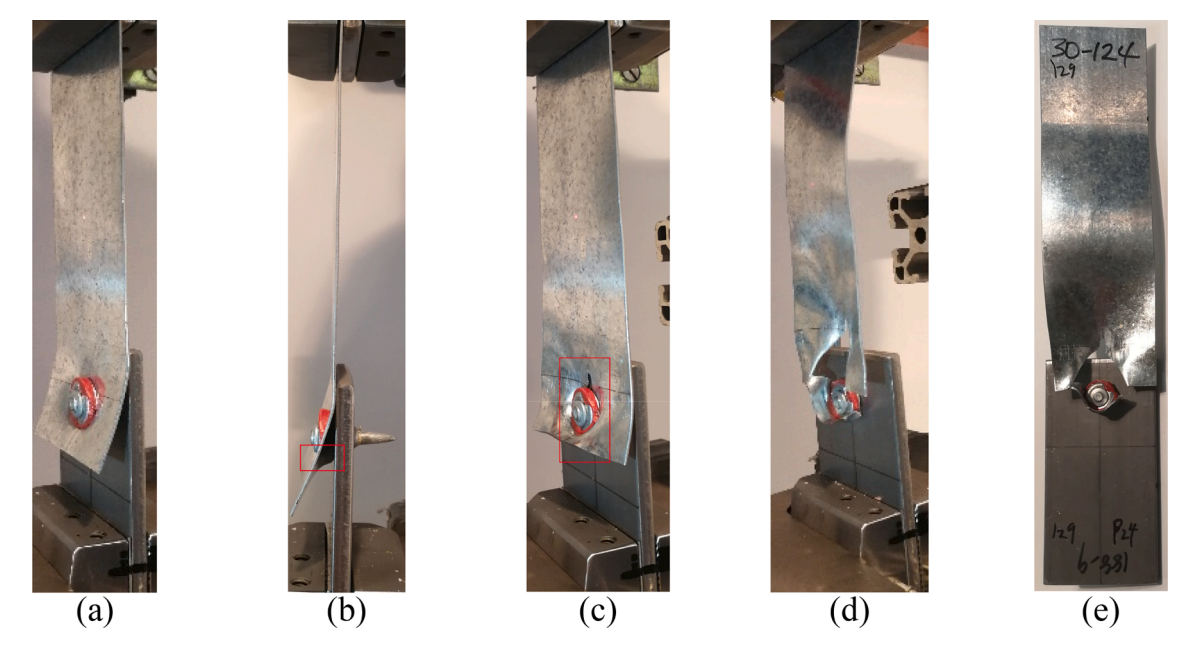


Fig. 10. Deformation and failure of a test in the "188-24-30" test series. (a) Peak strength level front view, (b) Peak strength level side view, (c) 80% post-peak strength level, (d) Post-test front view, (e) Post-test face-on view.

(b). Pull-through with bearing and shear rupture failure is triggered after bearing initiates which can be seen obviously in Fig. 11(d) and 11(e). The demand on the screw is predominantly shear with a small amount of tension. Bending of the thin steel sheet ply is initialized by the screw prying before the peak force level and develops throughout the test. No steel plate deformation is observed.

4.4. Force-displacement response

All the monotonic connection test results are presented in Fig. 12, the standard configuration "97-12-30" monotonic connection test result referenced from the complete test report [16] is also plotted herein for direct cross comparison. Response of all the double sided shear connection test series are provided in Fig. 13 and the response of single sided shear test series are presented in Fig. 14. Nonlinearity is observed

in the force-displacement response, overall trends are similar for most test series except the single sided shear connection test series with #12 self-drilling screw "188-12-30".

The "97-12-30-97" test series responses summarized and shown in Fig. 13(a) are representative of double sided shear connection configurations. Consistency in strength and post-peak behavior are observed in all the tests since the dominant failure modes are all bearing and further shear rupture. The same failures and consistency in the force-displacement response are also observed in other double sided shear configurations: "97-10-13-97", "97-10-19-97", "97-10-30-97", "97-24-30-97", "118-24-30-118". Further, "97-12-30-97" test series generates consistently higher strength than the strongest standard single sided shear configuration test series "97-12-30" in the test report [16], as shown in Fig. 14(d) (an average of 5.33 kN for the cyclic tests in "97-12-30" test series and 3.51 kN for the cyclic tests in "97-12-30" test

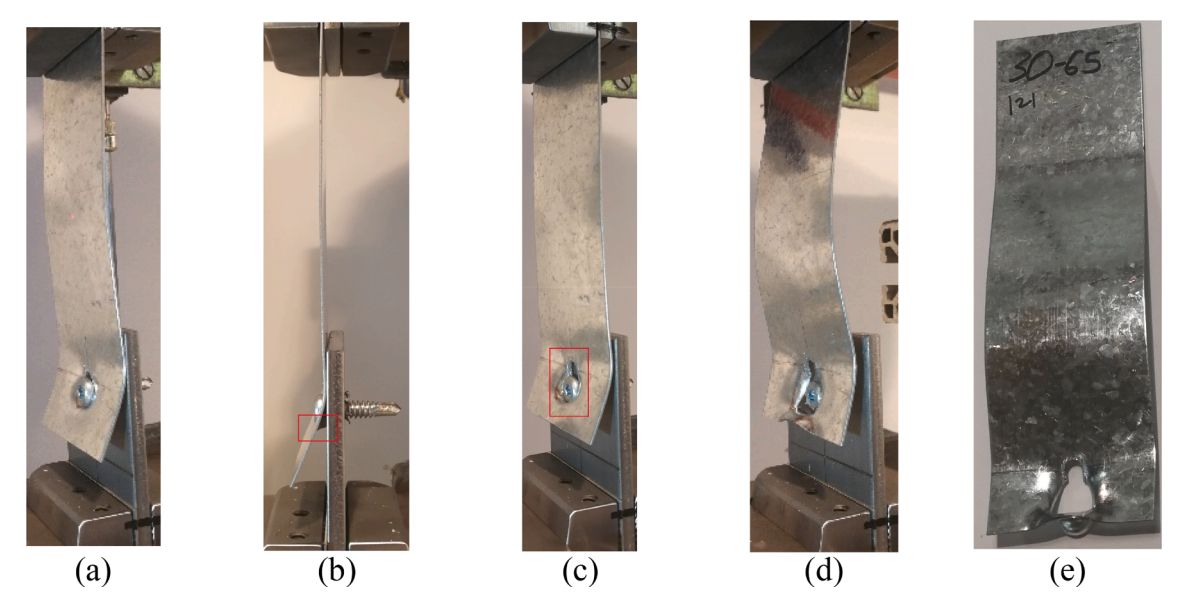


Fig. 11. Deformation and failure of a test in the "188-12-30" test series. (a) Peak strength level front view, (b) Peak strength level side view, (c) 80% post-peak strength level, (d) Post-test front view, (e) Post-test thin steel sheet ply face-on view.

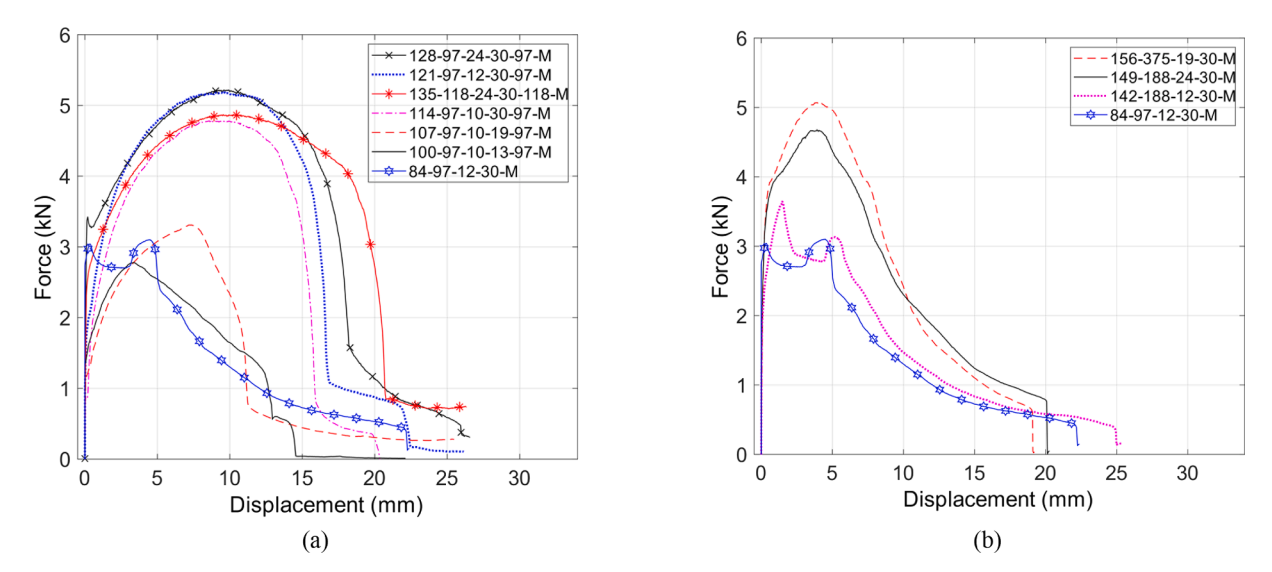


Fig. 12. Force-displacement curves of the monotonic test in each test series. (a) All the double sided shear monotonic tests, (b) All the single sided shear monotonic tests.

series). These results underpin the mid-ply shear wall tests and demonstrate specifically why the mid-ply configuration is highly favorable and, if it can be utilized in CFS framed steel sheet shear walls, provides a significantly improved strength and ductility for steel sheet systems.

The similar force-displacement responses are observed in single sided shear connection with PAF test series "188-24-30", as shown in Fig. 14(a). "188-24-30" test series generates consistently high average strength (4.88 kN) since the dominant failure modes are bearing and shear rupture. Consistency in strength and post-peak behavior are observed in all the tests. The same failures and strength consistency are also observed in the "375-19-30" test series. However, when a #12 self-drilling screw is adopted, such as "188-12-30" test series shown in Fig. 14(c), the force-displacement response sees variability in tests with different sheet buckling directions, which is because of the strength difference of pull-through and shear rupture limit states seen in the tests. This is similar to the standard single sided shear configuration test series "97-12-30" presented in Fig. 14(d) referenced from the complete test

report [16]. Compared with "188-24-30" test series, most tests in the "188-12-30" test series feature lower strength since the pull-through failure is triggered after the bearing is initiated. Thus, the efficient installation and superior performance of the PAF connections may be worth pursuing for thicker framing members – this has also been observed in cyclic tests on deck attached to thicker framing with PAF vs. screws [8,9].

Adopting two outer thick steel framing plies sandwiching one inner thin steel sheet ply to develop higher connection shear strength does work better than the normal single-sided shear configuration, which aligns with the higher shear wall strengths reported in the literature for this configuration [3–6]. However, thicker framing itself, such as in the "188-12-30" series, does not result in higher connection strength. This is within expectation since the stronger framing design concept aims to increase the stud axial capacity rather than increase the shear wall lateral resistance. However, adopting thicker framing steel with appropriate fasteners such as PAFs (or perhaps even screws with washers) can contribute to the fastener strength, as observed in the comparison

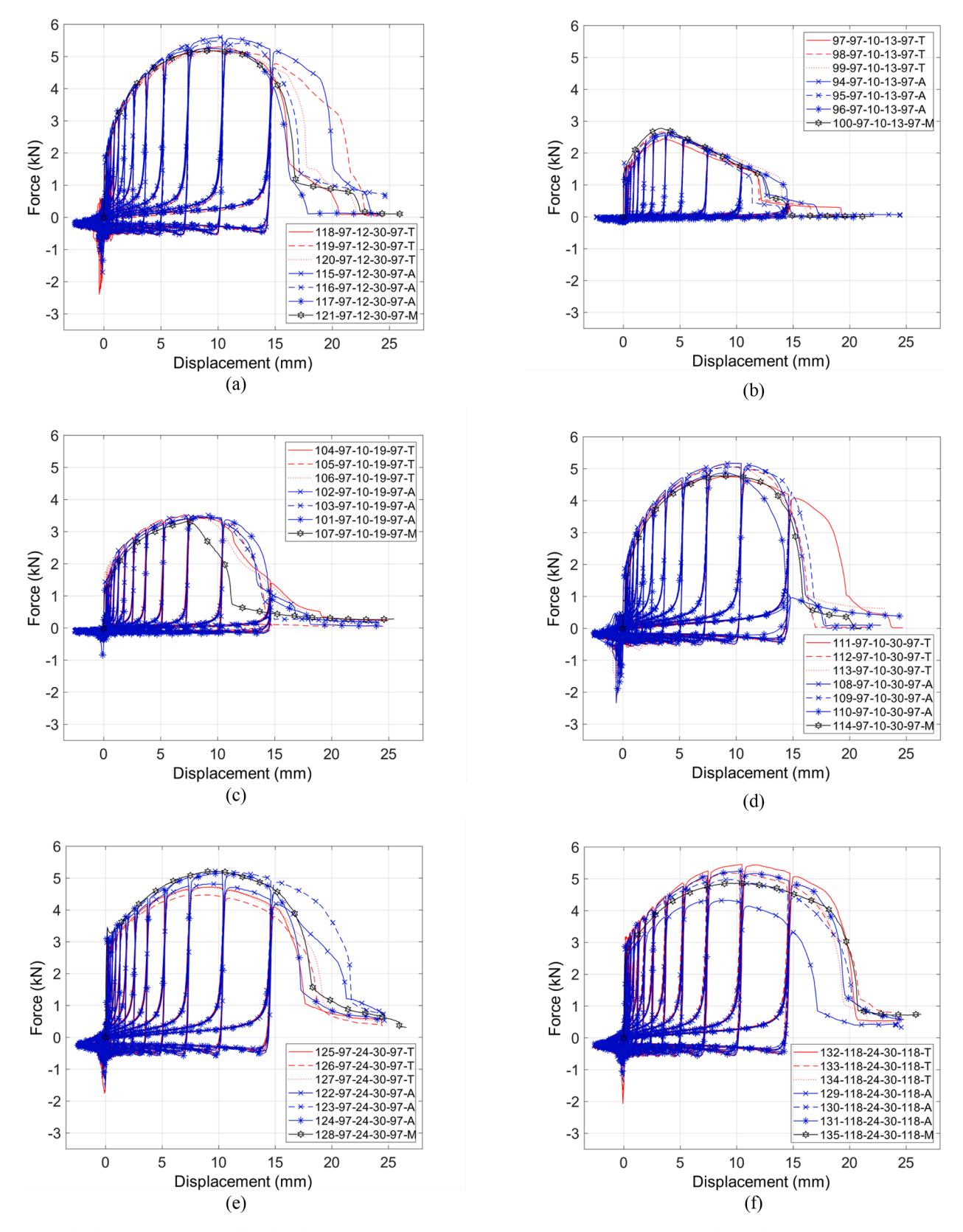


Fig. 13. Force-displacement curves of double sided shear connection test series. (a) "97-12-30-97" test series (0.76 mm sheet), (b) "97-10-13-97" test series (0.33 mm sheet), (c) "97-10-19-97" test series (0.48 mm sheet), (d) "97-10-30-97" test series (0.76 mm sheet), (e) "97-24-30-97" test series (0.76 mm sheet), (f) "118-24-30-118" test series (0.76 mm sheet).

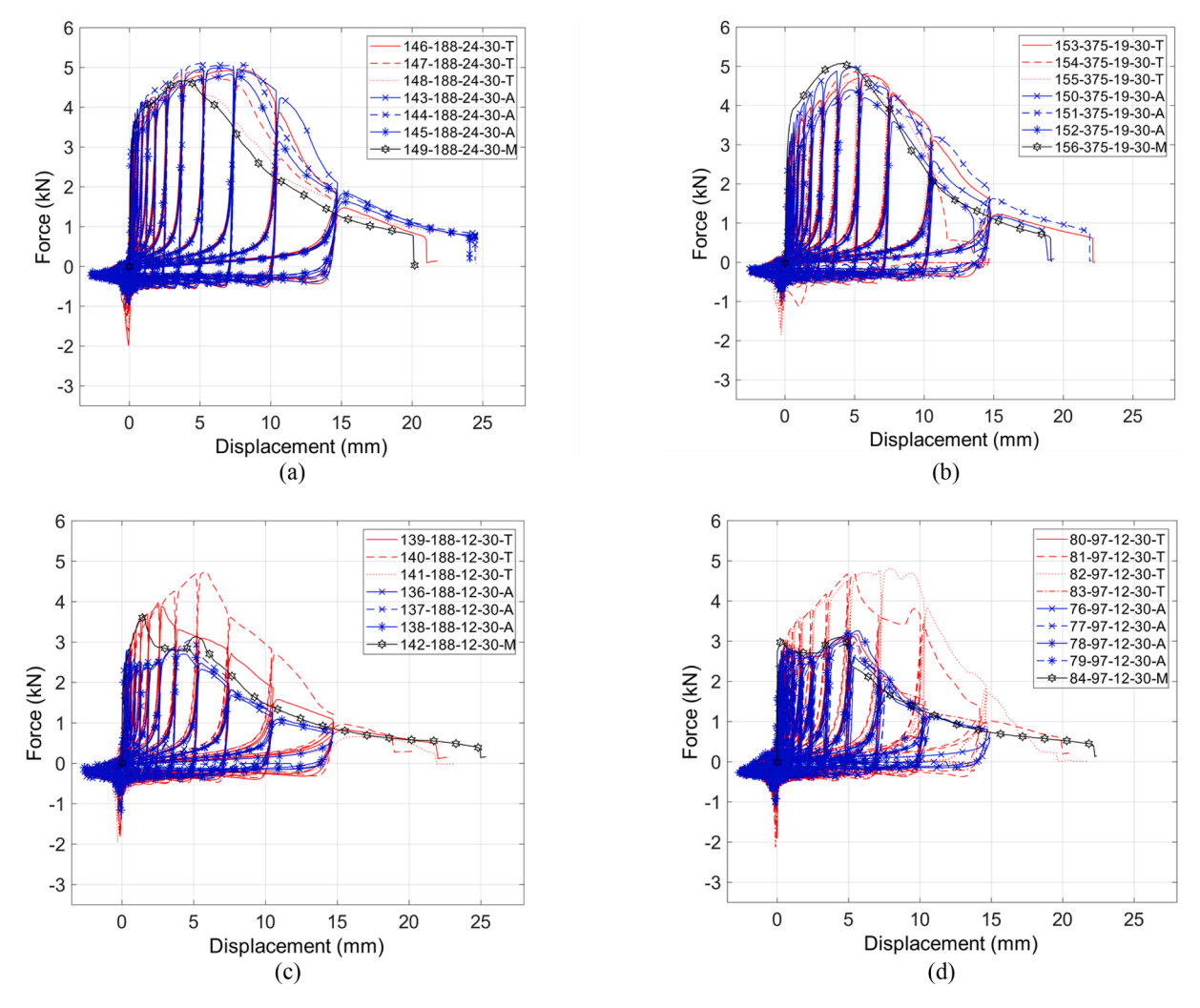


Fig. 14. Force-displacement curves of single sided shear connection test series. (a) "188-24-30" test series (0.76 mm sheet), (b) "375-19-30" test series (0.76 mm sheet), (c) "188-12-30" test series (0.76 mm sheet), (d) "97-12-30" test series in the test report [16] (0.76 mm sheet).

between "188-24-30" and "97-12-30" test series (39% increase in the average strength). This is because the enlarged PAF head design increases the moment-resisting arm of the connection and limits the fastener tilting and thin sheet steel ply bending deformation around the fastener head area. As a result, the in-plane shear slot deformation

similar to the double sided shear fastener connection configuration's effects can be observed in the connection with PAF. The relationship between force and lateral displacement of the center line at thin steel sheet was also recorded in the test report [16]. Compression displacement of 2.54 mm typically resulted in lateral deformation at center of

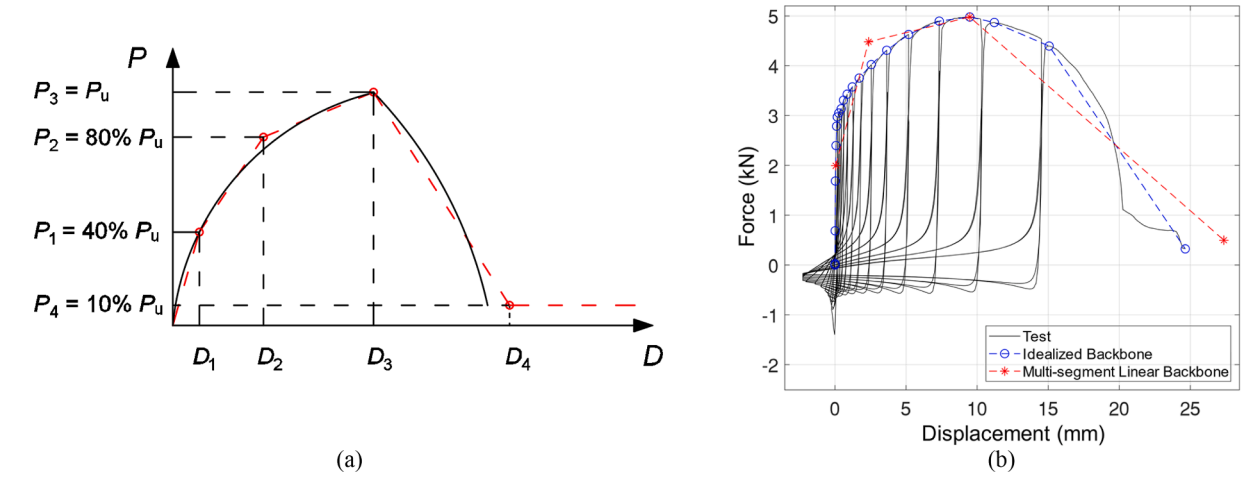


Fig. 15. Backbone data characterization based on equivalent cumulative energy dissipation. (a) Test data characterization diagram, (b) Example characterization for a test in the "97-12-30-97" test series.

the thin sheet up to 10.16 mm in elastic range and up to 30.48 mm when the plastic hinge developed.

4.5. Connection behavior characterization

A four-segment linear backbone phenomenological model consistent with the Pinching4 material model in OpenSees [26] is utilized for idealizing the test results to provide a convenient means to implement the tested connections in models. The model is fit by balancing energy between the linear segment model and the nonlinear tension side test results. The developed modeling parameters $(D_1, P_1; D_2, P_2; D_3, P_3; D_4, P_4)$ as depicted in Fig. 15(a) are meant for supporting numerical simulation where the nonlinear (hysteretic) fastener response is needed, e.g., in a shear wall simulation. An example characterization is provided for the "97-12-30-97" (double shear) test series in Fig. 15(b).

The averaged cyclic test data, and monotonic test data, for each test series is provided in Table 5. The fitted multi-segment linear backbone results for each individual test are provided in [16].

To assess the ductility of different fastener connection configurations, two ductility indices $\mu_1 = D_{80\%}/D_y$ and $\mu_2 = D_u/D_y$ are introduced herein. As presented in Fig. 16(a), D_v implies the displacement level

calculated based on the initial stiffness and peak force, $D_{80\%}$ represents the post-peak displacement corresponding to 80% peak force, D_u refers to the displacement level matching with 10% peak force level in the post-peak region. The averaged ductility index values of cyclic tests and the ductility index values of monotonic test for each test series are summarized in Table 6 and the averaged indices together with standard deviation values are plotted in Fig. 16(b). Large variation is seen in the test series "97-10-13-97" and "97-10-19-97". The index μ_1 is observed to be more consistent across different test series than index μ_2 since D_u depends on the test ending deformation, D_u can be large if the specimen experiences a complete disengagement. All the test series demonstrate reasonably high levels of ductility with index μ_1 featuring a minimum of 15 and an average of 43.

Utilizing the index μ_1 to discuss the results, the single sided shear connection test series "188-24-30" with X-HSN-24 PAF demonstrates systematically high ductility index (average of 76). The double sided shear connection test series "97-24-30-97" and "118-24-30-118" with X-HSN-24 PAF also feature high ductility indices (average of 91). This may be in part because the shank nominal diameter of the X-HSN-24 PAF is smaller than a #8 self-drilling screw and smaller shank diameter may result in more extensive deformation at the same force level.

Table 5Monotonic test and averaged cyclic test four-point backbone values.

Test series	Load type	D_1 (mm)	D_2 (mm)	D_3 (mm)	D_4 (mm)	P_1 (kN)	P_2 (kN)	P_3 (kN)	P_4 (kN)
97-10-13-97	Monotonic	0.03	1.19	3.40	16.46	1.11	2.39	2.78	0.28
	Cyclic	0.12	1.48	3.80	17.69	1.04	2.17	2.58	0.26
97-10-19-97	Monotonic	0.36	2.72	7.37	15.80	1.33	2.80	3.31	0.33
	Cyclic	0.30	2.53	8.53	19.04	1.38	3.02	3.46	0.35
97-10-30-97	Monotonic	0.51	3.02	9.68	20.09	1.91	4.18	4.79	0.48
	Cyclic	0.34	3.00	9.38	23.21	2.01	4.36	5.02	0.50
97-12-30-97	Monotonic	0.36	2.74	9.60	22.83	2.07	4.54	5.19	0.52
	Cyclic	0.35	3.09	10.01	26.04	2.13	4.66	5.33	0.53
97-24-30-97	Monotonic	0.05	2.82	9.93	25.40	2.09	4.71	5.22	0.52
	Cyclic	0.06	2.40	9.56	27.32	1.94	4.37	4.85	0.49
118-24-30-118	Monotonic	0.08	2.62	10.29	28.27	1.95	4.31	4.87	0.49
	Cyclic	0.06	2.65	9.89	27.36	2.03	4.53	5.07	0.51
188-12-30	Monotonic	0.03	0.56	1.45	18.03	1.46	3.13	3.65	0.36
	Cyclic	0.10	0.97	4.19	15.10	1.36	2.85	3.41	0.34
188-24-30	Monotonic	0.05	0.58	3.91	17.75	1.87	4.02	4.68	0.47
	Cyclic	0.05	0.95	5.77	20.08	1.95	4.27	4.89	0.49
375-19-30	Monotonic	0.10	0.91	4.17	16.54	2.03	4.51	5.08	0.51
	Cyclic	0.15	1.58	5.29	16.47	1.87	4.06	4.67	0.47

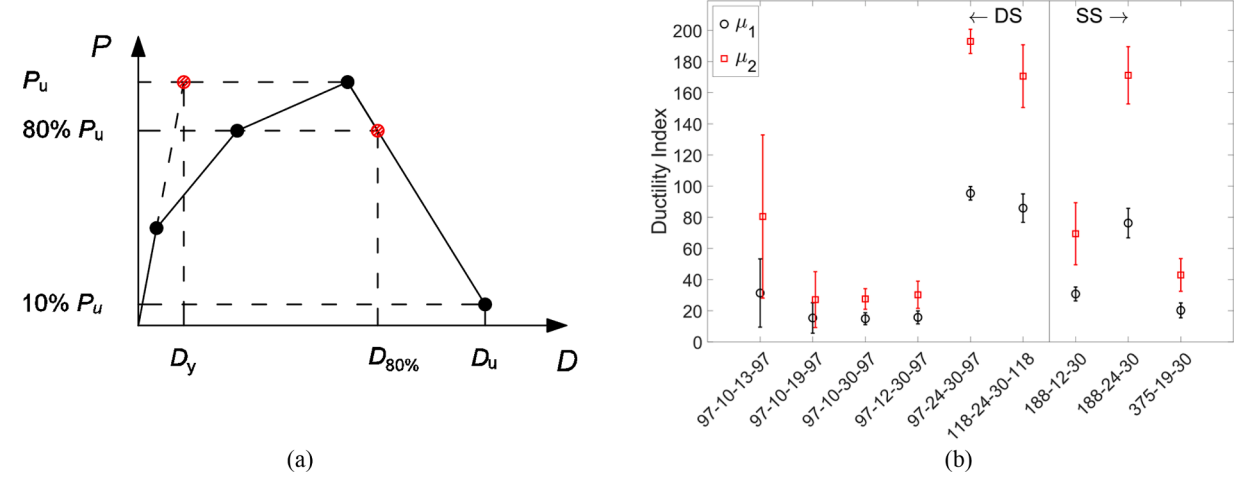


Fig. 16. Test ductility index. (a) Test displacement level diagram, (b) Test ductility index comparison.

Table 6
Monotonic test and averaged cyclic test ductility data and indices.

Test series	Load type	D_{y} (mm)	$D_{80\%}$ (mm)	D_{u} (mm)	μ_1		μ_2		
					Average	CoV	Average	CoV	
97-10-13-97	Monotonic	0.09	6.31	16.45	73.76	_	192.29	_	
	Cyclic	0.30	6.89	17.69	31.39	0.58	80.49	0.54	
97-10-19-97	Monotonic	0.89	9.24	15.80	10.39	_	17.77	-	
	Cyclic	0.75	10.87	19.04	15.37	0.54	27.16	0.56	
97-10-30-97	Monotonic	1.28	11.99	20.09	9.34	_	15.64	-	
	Cyclic	0.85	12.45	23.21	14.88	0.24	27.57	0.23	
97-12-30-97	Monotonic	0.88	12.54	22.84	14.28	_	26.01	-	
	Cyclic	0.87	13.58	26.04	15.75	0.25	30.27	0.28	
97-24-30-97	Monotonic	0.14	13.37	25.39	98.09	_	186.31	-	
	Cyclic	0.14	13.50	27.32	95.40	0.08	192.92	0.07	
118-24-30-118	Monotonic	0.19	14.28	28.28	74.96	-	148.47	_	
	Cyclic	0.16	13.78	27.36	85.90	0.19	170.61	0.21	
188-12-30	Monotonic	0.09	5.14	18.03	57.95	-	203.24	_	
	Cyclic	0.24	6.62	15.10	30.78	0.23	69.46	0.40	
188-24-30	Monotonic	0.14	6.99	17.76	50.35	_	127.85	_	
	Cyclic	0.12	8.95	20.08	76.29	0.26	171.15	0.23	
375-19-30	Monotonic	0.24	6.91	16.54	28.96	_	69.32	_	
	Cyclic	0.39	7.77	16.47	20.25	0.26	42.99	0.27	

5. Code strength predictions

Bearing, pull-through, and shear rupture are the failure modes observed in this research. For bearing in screwed connections the provisions of J4.3.1 in AISI S100-16 [14] apply and is governed by Eq. (1).

$$P_{nv} = 2.7t_1 dF_{u1} (1)$$

where t_1 and $F_{\rm u1}$ are the thickness and ultimate strength of the steel sheet in contact with the screw head (always the thinner sheet ply in the tests here), and d is the screw diameter. In addition, for Eq. (1) to apply t_2/t_1 must be larger than 2.5 where t_2 is the thickness of the steel sheet not in contact with the screw head (the framing ply in the tests here). Eq. (1) can be further generalized to account for single or double side shear and for PAF connections if provisions in J3.3.1 and J5.3.2 in AISI S100-16 [14] are employed resulting in a generalized expression Eq. (2) for bearing.

$$P_{nv} = m_f \alpha_b t_1 dF_{u1} \tag{2}$$

where modification factor for type of bearing connection m_f equals to 1.00 for single shear and 1.33 for double shear, and the strength adjustment factor α_b equals to 2.7 for screwed connections and 3.7 for

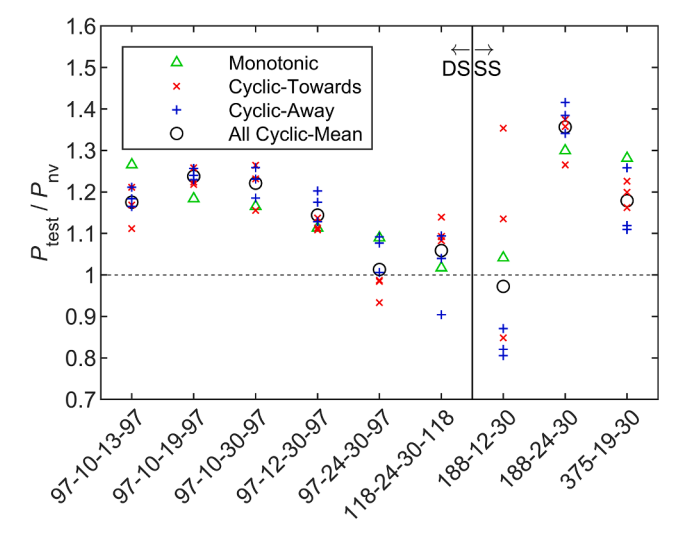


Fig. 17. Ratio of test strength to bearing strength across specimens.

PAF connections in this study. Pull-through follows bearing and a separate strength check is not considered here.

Strength of the shear rupture limit state is predicted by provisions of J6.1 in AISI S100-16 [14], shown in Eq. (3).

$$P_{net} = 0.6F_{u1}2t_1e_{net} (3)$$

where e_{net} is the clear distance between end of material and edge of the fastener hole.

As presented in Fig. 17, ratio of test strength to bearing strength prediction across specimens and the mean ratio of the cyclic tests within each test series are visualized. The test-to-predicted ratios of all the double shear configuration (DS) test series demonstrate mean value 1.14 and coefficient of variation (CoV) 0.08 while mean value is 1.17 with CoV equal to 0.18 for all the single shear configuration (SS) test series, implying that the shear strength limited by the bearing provision together with the modification factor for double shear configuration and strength adjustment factor for PAF in the AISI S100-16 [14] can provide reasonable/conservative fastener shear strength predictions. As shown in Fig. 18, the test and prediction strength values are normalized by $t_1F_{11}w$, with specimen width w of 50.8 mm, it is observed that the

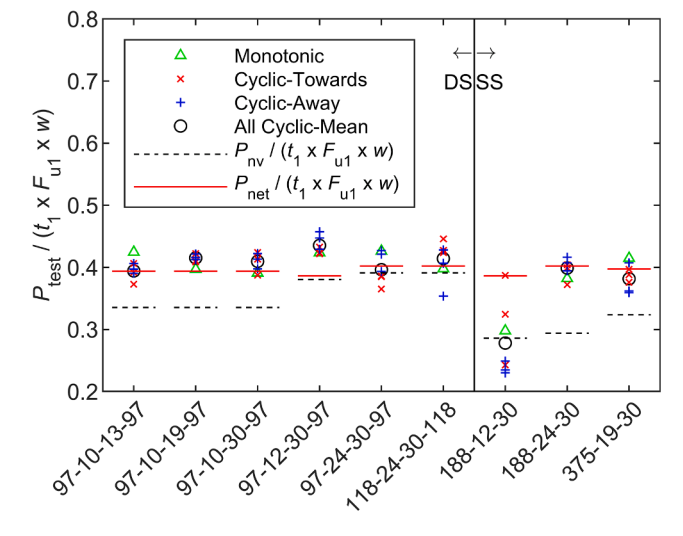


Fig. 18. Ratio of test strength to ultimate sheet strength for comparison to shear rupture coefficient.

normalized average test strength of all the test series lies close to the normalized shear rupture provision prediction and reasonably higher than the normalized shear strength limited by bearing provision except "188-12-30". This aligns with the test observation that the limit states of these tests are bearing and shear rupture. The normalized average test strength of "188-12-30" test series is close to the normalized shear strength limited by bearing. This can be supported by the test observation that most tests in this test series demonstrate mainly bearing leading limit states.

6. Conclusions

Isolated lap-shear fastener tests, appropriate for characterizing the cyclic performance of connectors utilized in novel cold-formed steel (CFS) framed steel sheet sheathed shear walls, are completed and summarized herein. Two classes of new shear walls motivate the testing: mid-ply shear walls that sandwich the perimeter of the thin steel sheet sheathing between framing members and thus when fastened together provide a double shear connection, and heavy steel sheet shear walls that use hollow structural sections (HSS) for the chord studs and power actuated fasteners (PAFs) to connect the perimeter steel sheet sheathing back to the HSS framing. The testing configuration is designed, in an isolated single fastener shear test, to mimic key features of the perimeter fasteners in these steel sheet sheathed shear walls. Specimens are subject to cycles of displacement that first buckle the thin steel sheet sheathing and potentially places prying on the fastener head, then second reverses direction in progressively larger displacements that are resisted by bearing of the fastener (screw or PAF) against the thin steel sheet. The strength of the tested connections agrees well with AISI S100, and the ductility of the connections, which respond primarily in bearing, is quite good. A multi-linear backbone response curve, appropriate for use in models of perimeter connectors for CFS-steel sheet sheathed shear walls, is developed from the testing and provided. The model provides a means to expand on the limited shear wall testing conducted to date and develop guidance for engineers interested in specifying these new shear wall configurations.

7. Data availability statement

Some or all data, models, or code generated or used during the study are available from the corresponding author by request, which include experimental raw data and results.

CRediT authorship contribution statement

Zhidong Zhang: Conceptualization, Data curation, Investigation, Methodology, Software, Visualization, Writing - original draft, Writing - review & editing. Amanpreet Singh: Investigation, Methodology. Fani Derveni: Investigation, Methodology, Writing - review & editing. Shahabeddin Torabian: Software, Investigation. Kara D. Peterman: Methodology, Visualization, Supervision, Writing - review & editing. Tara C. Hutchinson: Methodology, Visualization, Supervision. Benjamin W. Schafer: Conceptualization, Funding acquisition, Supervision, Methodology, Resources, Writing - review & editing.

Declaration of Competing Interest

The authors declare that they have no known competing financial interests or personal relationships that could have appeared to influence the work reported in this paper.

Acknowledgement

This work is part of the research project Seismic Resiliency of Repetitively Framed Mid-Rise Cold-Formed Steel Building (CFS-NHERI) which is supported by the National Science Foundation under Grant No.1663348 and No.1663569. Test materials provided by ClarkDietrich and Hilti, Inc. are gratefully acknowledged. The tests conducted herein were assisted by Gbenga Olaolorun, Joel John, Boyu Qian and Nick Logvinovsky, the authors would like to express gratitude to their great help. Any opinions, findings, and conclusions or recommendations expressed in this material are those of the authors and do not necessarily reflect the views of the sponsors.

References

- Madsen RL, Castle TA, Schafer BW. Seismic design of cold-formed steel lateral loadresisting systems: a guide for practicing engineers. NEHRP Seismic Design Technical Brief No. 12; 2016.
- [2] Singh A, Wang X, Torabian S, Hutchinson TC, Peterman KD, Schafer BW. Seismic performance of symmetric unfinished CFS In-line wall systems. In: Structures Congress; 2020. p. 629–42.
- [3] Santos V, Rogers CA. Higher capacity cold-formed steel sheathed and framed shear walls for mid-rise buildings: part 1. Research Report RP17-5. Montreal, QC: Dept. of Civil Engineering and Applied Mechanics, McGill University; 2017.
- [4] Brière V, Rogers CA. Higher capacity cold-formed steel sheathed and framed shear walls for mid-rise buildings: part 2. Research Report RP17-6. Montreal, QC: Dept. of Civil Engineering and Applied Mechanics, McGill University; 2017.
- [5] Brière V, Santos V, Rogers CA. Cold-formed steel centre-sheathed (mid-ply) shear walls. Soil Dyn Earthquake Eng 2018;114:253–66.
- [6] Wu JC. Performance of centre-sheathed cold-formed steel framed shear walls phase 2. PhD dissertation. Montreal, QC: McGill University; 2019.
- [7] Shi Y, Torabian S, Schafer BW, Easterling WS, Eatherton MR. Sidelap and structural fastener tests for steel deck diaphragms. Proceedings of the International Specialty Conference on Cold-Formed Steel Structures, St. Louis, MO. 2018.
- [8] Torabian S, Schafer BW. Cyclic performance and characterization of steel deck connections. Research report; 2017.
- [9] Torabian S, Schafer BW. Cyclic Experiments on Sidelap and Structural Connectors in Steel Deck Diaphragms. J Struct Eng 2021;147(4).
- [10] Daudet RL, LaBoube RA. Shear behavior of self drilling screws used in low ductility steel. Proc. 13th international specialty conference on cold-formed steel structures. 1996.
- [11] Koka EN, Yu WW, LaBoube RA. Screw and welded connection behavior using structural grade 80 of A653 steel (a preliminary study). Center for Cold-Formed Steel Structures Library; 1997.
- [12] AISI-S400-15. North American standard for seismic design of cold-formed steel structural systems. In AISI-S400. Washington, D.C.: American Iron and Steel Institute; 2015.
- [13] Yanagi N, Yu C. Effective strip method for the design of cold-formed steel framed shear wall with steel sheet sheathing. J Struct Eng 2014;140(4).
- [14] AISI-S100-16. North American specification for the design of cold-formed steel structural members. Washington, D.C.: American Iron and Steel Institute; 2016.
- [15] AISI S905-13. Test standard for cold-formed steel connections. Washington, D.C.: American Iron and Steel Institute; 2013.
- [16] Zhang Z, Schafer BW. Cyclic performance of steel sheet connections for CFS steel sheet shear walls. Research report CFSRC R-2020-06, cold-formed steel research consortium; 2020.
- [17] Rizk R, Rogers CA. Higher strength cold-formed steel framed/steel shear walls for mid-rise construction. Research Report RP17-4. Montreal, QC: Dept. of Civil Engineering and Applied Mechanics, McGill University; 2017.
- [18] Yu C, Vora H, Dainard T, Tucker J, Veetvkuri P. Steel sheet sheathing options for CFS framed shear wall assemblies providing shear resistance. Report No. UNT-G76234. Denton, TX: Department of Engineering Technology, University of North Texas; 2007.
- [19] Tao F, Chatterjee A, Moen CD. Monotonic and cyclic response of single shear cold-formed steel-to-steel and sheathing-to-steel connections. Research Report No. CE/VPI-ST-16/01. Blacksburg, VA: Virginia Tech; 2016.
- [20] Federal Emergency Management Agency (FEMA). FEMA 461, Interim protocols for determining seismic performance characteristics of structural and nonstructural components through laboratory testing. Washington, D.C.: Federal Emergency Management Agency; 2007.
- [21] Zhang Z, Schafer BW. Simulation of steel sheet sheathed cold-formed steel framed shear walls. Proc. annual stability conference-structural stability research council. 2019.
- [22] ASTM-E8/E8M-13a. Standard test methods for tension testing of metallic materials. West Conshohocken, PA: American Society for Testing and Materials; 2013.
- [23] Torabian S, Zheng B, Shifferaw Y, Schafer BW. Direct strength prediction of coldformed steel beam-columns. Research report RP16-3. AISI; 2016.
- [24] AISI S907-17. Test Standard for Determining the Strength and Stiffness of Cold-Formed Steel Diaphragms by the Cantilever Test Method. Washington, D.C.: American Iron and Steel Institute; 2017.
- [25] AISI S917-17. Test Standard for Determining the Fastener-Sheathing Local Translational Stiffness of Sheathed Cold-Formed Steel Assemblies. Washington, D. C.: American Iron and Steel Institute; 2017.
- [26] Mazzoni S, McKenna F, Scott MH, Fenves GL. OpenSees command language manual, vol. 264. Pacific Earthquake Engineering Research (PEER) Center; 2006.